

The mechanism of *Klebsiella pneumoniae* nitrogenase action

Simulation of the dependences of H₂-evolution rate on component-protein concentration and ratio and sodium dithionite concentration

Roger N. F. THORNELEY and David J. LOWE

A.F.R.C. Unit of Nitrogen Fixation, University of Sussex, Brighton BN1 9RQ, U.K.

(Received 6 June 1984/Accepted 24 August 1984)

The rate constants from Table 1 and Scheme 2 of Lowe & Thorneley [(1984) *Biochem. J.* 224, 877–886] were used to simulate the rate of H₂ evolution, under various conditions, from nitrogenase isolated from *Klebsiella pneumoniae*. These rates depend on both the ratio and concentrations of the MoFe protein and Fe protein that comprise nitrogenase. The simulations explain the shapes of 'protein titration' and 'dilution effect' curves. The concept of an apparent K_m for the reductant Na₂S₂O₄ is shown to be invalid, since the dependence of H₂-evolution rate on the square root of S₂O₄²⁻ concentration is not hyperbolic and depends on the ratio and absolute concentrations of the MoFe protein and Fe protein.

In the four previous papers in this series (Thorneley & Lowe, 1983, 1984; Lowe & Thorneley, 1984a,b) we developed a comprehensive kinetic model for the mechanism of nitrogenase action. A rigorous test of this model is whether it is capable of simulating the dependence of the rate of H₂ evolution on the concentration and ratio of the two proteins, the MoFe protein (Kp1) and the Fe protein (Kp2), that comprise nitrogenase. Such dependences form the basis of the standard assay used to determine the specific activities of the MoFe protein and Fe protein and are often referred to as 'titration curves' (Eady *et al.*, 1972; Emerich *et al.*, 1981). The maximum rate of H₂ evolution (or C₂H₂ reduction) is used to calculate the specific activity. Because of the limitations of substrate supply, product inhibition and the time required for syringe additions to start and terminate assays, protein concentrations in the range 0.5–5 μM are commonly used for these assays. However, for rapid-quench experiments designed to investigate the pre-steady-state phase of product, formation (Lowe & Thorneley, 1984a; Thorneley & Lowe, 1984), protein concentrations in the range 10–100 μM need to be used. The specific activities calculated for H₂ evolution from the steady-state rate at 10 s showed that at these high protein concentrations nitrogenase is inhibited.

Alternatively, if low concentrations (<0.5 μM) of nitrogenase component proteins are used, a decrease in specific activity is observed as the total protein concentration decreases. This is often referred to as the 'dilution effect' (Mortenson, 1964).

Thus three classes of experiment, namely dilution effect, titration curves and pre-steady-state rapid quench, have provided data that show a complex dependence of H₂-evolution rate on the absolute concentrations and ratio of the Fe protein and MoFe protein. In the present paper we explain these kinetics and show how the dependences can be simulated by using Scheme 2 and the rate constants in Table 1 of Lowe & Thorneley (1984a). We have not allowed any of the values of these rate constants to vary in order to decrease deviation between the simulations and the experimental points.

Methods and materials

Protein preparation

Nitrogenase component proteins (Kp1 and Kp2) were purified and characterized as previously described (Lowe & Thorneley, 1984a).

Assay procedure and kinetic analysis

The steady-state rates of H₂ formation were determined as previously described (Lowe & Thorneley, 1984b), with medium containing 9 mM-

Abbreviations used: Kp1 and Kp2, MoFe-containing protein and Fe-containing protein components respectively of *Klebsiella pneumoniae* nitrogenase.

ATP, 10mM-MgCl₂, 25mM-Hepes [4-(2-hydroxyethyl)-1-piperazine-ethanesulphonic acid]/NaOH buffer, pH 7.4, and 10mM-Na₂S₂O₄ except where stated. The concentrations of Kp1 and Kp2 are given in the legends or in the text. The duration of the assays was varied (usually in the range 5–40min) to ensure that the time course for H₂ formation was linear and to optimize the yield of H₂. It was not possible to maintain a constant rate of H₂ evolution at the low S₂O₄²⁻ concentrations shown in Fig. 5, since a significant amount of the dithionite was consumed during the course of the assay. Therefore the data points and the simulated curves in Fig. 5 represent the total number of nmol of H₂ formed after 1 or 5min and initial S₂O₄²⁻ concentration.

The data at high protein concentrations (Fig. 2) were obtained by using a rapid-quench technique described by Lowe & Thorneley (1984a) and conventional assays of 5–10 s duration. The latter assay procedure, involving rapid manual syringe additions of premixed Kp1 and Kp2 proteins (0.01–0.2 ml) to initiate the reaction and 40% (w/v) trichloroacetic acid (0.1 ml) to terminate the assay, was originally developed to check that the inhibition of H₂ evolution observed at high protein concentrations in pre-steady-state H₂-evolution studies (Lowe & Thorneley, 1984a) was a genuine effect and not due to protein inactivation. The glass vials (2.3 ml) used for these assays were fitted with rubber closures through which syringe additions could be made; they contained 0.4 ml of reaction mixture and enzyme under Ar. After completion of the assay, the vial was inverted and shaken vigorously for 15 min to allow equilibration of H₂ between the liquid and gas phase. A gas sample (0.3 ml) was used for H₂ analysis by vapour-phase chromatography as described by Dilworth & Thorneley (1981).

The simulated curves were obtained by using Scheme 2, the rate constants in Table 1 and the computing procedure described in Lowe & Thorneley (1984a).

Results and discussion

Dependence of the rate of H₂ evolution on protein concentration (dilution effect)

The dilution effect (see the introduction) occurs when the concentration of nitrogenase component proteins is decreased below 0.5 μM, while a constant Fe protein/MoFe protein ratio protein is maintained. Thorneley *et al.* (1975) analysed kinetic data for C₂H₂ reduction at 30°C by assuming that reversible complex-formation occurs between Kp2 and Kp1 and that the substrate-reduction activity was associated with the complexed proteins. Thus the 'dilution effect' was

explained as a mass-action effect on this equilibrium ($K = 2.0 \times 10^7 \pm 0.6 \times 10^7 \text{ M}^{-1}$ at 30°C).

A more rigorous analysis of this effect is now possible as a consequence of studies on the kinetics of the oxidation–reduction of Kp2 (Thorneley & Lowe, 1983) and the substrate-reduction cycle (Scheme 2 of Lowe & Thorneley, 1984a). Data were obtained for H₂ evolution at 23°C as a function of [Kp1 + Kp2] protein concentration at a constant [Kp2]/[Kp1] ratio of 4:1 (Fig. 1). C₂H₂ was not used as a substrate, for two reasons. Firstly, we have not yet fitted C₂H₂ reduction into our overall substrate-reduction scheme, and, secondly, we have evidence suggesting that C₂H₂ and its reduction product C₂H₄ may perturb the equilibria between Kp1 and Kp2 proteins.

The line through the data points in Fig. 1 is a simulation made by using the rate constants in Table 1 and Scheme 2 of Lowe & Thorneley (1984a). The simulation is sensitive to the value of k_{+1} but not to that of k_{-1} provided that $k_{-1} < 100 \text{ s}^{-1}$ (see the discussion in Lowe & Thorneley, 1984b). Thus the 'dilution effect' is due to the rate of association of reduced Kp2 (MgATP)₂ with Kp1[†] (k_{+1}) becoming rate-limiting at low protein concentrations. Because $k_{-1} \ll k_2$, the rapid pre-equilibrium treatment used by Thorneley *et al.* (1975) is not germane and the value of k_{+1}/k_{-1} cannot be deduced.

Inhibition of H₂ evolution at high protein concentration

Fig. 2 shows the rate of H₂ evolution (nmol/min per mg of Kp1) as a function of the Kp2 and Kp1

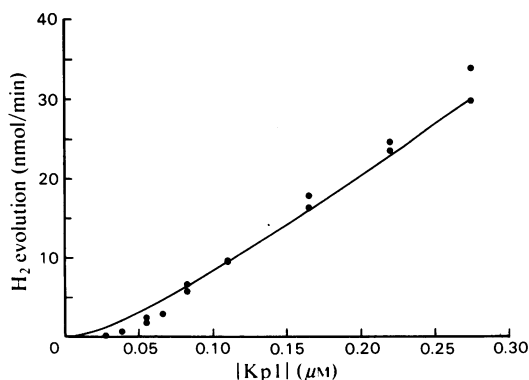


Fig. 1. Dilution effect: dependence of the rate of H₂ evolution on protein concentration at 23°C at pH 7.4. The data points were obtained by using the standard assay procedure described in the Methods and materials section. A constant [Kp2]/[Kp1] molar ratio of 4:1 was used. The continuous line is a simulation obtained by using the rate constants in Table 1 and Scheme 2 of Lowe & Thorneley (1984a).

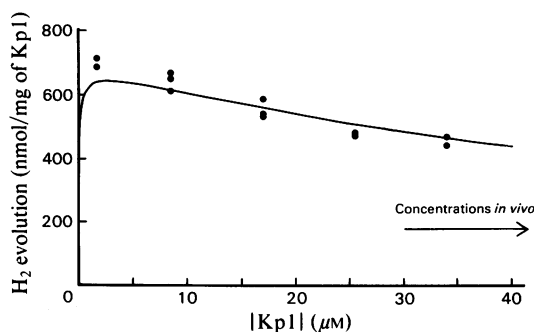


Fig. 2. Inhibition of H_2 evolution at high protein concentrations

The data points were obtained by using the 10s assay procedure described in the Methods and materials section. The $[Kp2]/[Kp1]$ molar ratio was 4:1 at all points, and the continuous line is a simulation obtained by using the rate constants in Table 1 and Scheme 2 of Lowe & Thorneley (1984a). The arrow indicates the range of nitrogenase concentrations present *in vivo*.

protein concentrations. The $[Kp2]/[Kp1]$ ratio was constant at 4:1. The line through the data points is a simulation made by using Scheme 2 and the rate constants in Table 1 of Lowe & Thorneley (1984a). As the total protein concentration increases, the specific activity of the Kp1 protein decreases.

The inhibition is due to the mass-action effect on the equilibrium between $Kp2_{ox}(\text{MgADP})_2$ and $Kp1^\dagger$ [k_{+3} and k_{-3} , Scheme 1 of Lowe & Thorneley (1984a)].

The dissociation of the complex $Kp2_{ox}(\text{MgADP})_2\text{-}Kp1^\dagger$ (k_{-3}) is rate-limiting at high protein concentrations when all other substrates are saturating (Thorneley & Lowe, 1983). The effective dissociation rate is given by eqn. (1):

$$\text{Rate} = k_{-3}[Kp2_{ox}(\text{MgADP})_2 - Kp1^\dagger] - k_3[Kp2_{ox}(\text{MgADP})_2][Kp1^\dagger] \quad (1)$$

In the absence of fast competing reactions, inhibition occurs when the second term becomes significant. Since $k_{-3} = 6.4\text{s}^{-1}$ and $k_3 = 4.4 \times 10^6\text{M}^{-1}\cdot\text{s}^{-1}$, steady-state concentrations of free $Kp2_{ox}(\text{MgADP})_2$ above $1\mu\text{M}$ are potentially inhibitory. The percentage of the total Kp2 protein that is present as $Kp2_{ox}(\text{MgADP})_2$ in the steady state depends *in vitro* on (a) the concentration of $\text{Na}_2\text{S}_2\text{O}_4$, (b) the $[Kp2]/[Kp1]$ ratio, and (c) the total concentrations of Kp2 and Kp1. In practice the equilibrium described by eqn. (1) is never in balance, since the reaction of Kp2 ($\text{MgATP})_2$ with free $Kp1^\dagger$ competes with k_3 . Hence the inhibition is only as great as would be expected from eqn. (1) when $k_{+1}[Kp2(\text{MgATP})_2] \ll k_3[Kp2_{ox}(\text{MgADP})_2]$.

The specific activity of Kp1 protein (nmol of H_2 /min per mg of Kp1) therefore depends on the $\text{S}_2\text{O}_4^{2-}$ concentration and the absolute protein concentration as well as the $[Kp2]/[Kp1]$ molar ratio used in the assay. Three overlapping ranges of $[Kp1 + Kp2]$ merit discussion. Firstly, when $[Kp1 + Kp2]$ is less than $1\mu\text{M}$, the dilution effect operates and the specific activity of Kp1 increases as the total protein concentration increases. In this region, k_{+1} is rate-limiting. Secondly, when $[Kp1 + Kp2]$ is $1\text{--}5\mu\text{M}$, provided that $[Kp2] \gg [Kp1]$ and all other substrates are saturating, k_{-3} is rate-limiting and the maximum specific activity for Kp1 is obtained. The concentrations of nitrogenase proteins that have normally been used for steady-state kinetic experiments, including the routine assay to determine the specific activities of the component proteins during isolation and purification, are in this concentration range (see the section below on titration curves).

Thirdly, when $[Kp1 + Kp2]$ is greater than $5\mu\text{M}$, k_{+3} can become significant and the specific activity of Kp1 decreases as the total concentration of protein increases. This is important, since high protein concentrations have been used to study the pre-steady-state kinetics of H_2 , N_2H_4 and $\cdot\text{NH}_3$ formation (Lowe & Thorneley, 1984a; Thorneley & Lowe, 1984). High protein concentrations are currently essential for obtaining data with spectroscopic techniques such as e.p.r., electron-nuclear double resonance, n.m.r., Mössbauer and extended X-ray-absorption fine structure. The analysis of spectroscopic data obtained with high concentrations of functioning nitrogenase (samples will generally be obtained by using a rapid-freeze technique in the time range 10ms–10s) will need to take this inhibition into account. The ability to simulate the time courses of the concentrations of the intermediate states of Kp2 and Kp1 in the pre-steady-state and steady-state reaction phases must enhance the chances of detecting, spectroscopically, intermediates such as the hydrido species proposed by Lowe & Thorneley (1984a).

Several species are capable of competing with $Kp2(\text{MgATP})_2$ for free $Kp1^\dagger$, and the resulting inhibition may be important in the regulation of activity *in vivo*. These species include $Kp2_{ox}(\text{MgADP})_2$, $Kp2_{ox}(\text{MgATP})_2$, $Kp2(\text{MgADP})_2$ and any inactive forms of Kp2 that can bind to $Kp1^\dagger$.

The concentration of nitrogenase component proteins *in vivo* is approx. $100\mu\text{M}$ (Eady *et al.*, 1978; Roberts *et al.*, 1978; Hennecke & Shanmugam, 1979). Lowe & Thorneley (1984a) discussed the advantages of nitrogenase being a slow enzyme present at high concentration in terms of optimizing N_2 reduction relative to H_2 evolution. This high concentration can cause nitrogenase activity

to be inhibited *in vivo*. The degree of inhibition can be modulated in three ways. Firstly, the steady-state concentration of the inhibitor $Kp2_{ox.}(MgADP)_2$ is determined by the electron-transfer rate from the donor (flavodoxin or ferredoxin) and the concentration of the donor in the reduced state. Secondly, the concentration of the inhibited complex $Kp2_{ox.}(MgADP)_2-Kp1^\dagger$ depends on the concentration of reduced $Kp2 (MgADP)_2$ or $Kp2-(MgATP)_2$. These reduced Fe protein species compete effectively (k_{+5} and k_{-5} ; Thorneley & Lowe, 1983) with $Kp2_{ox.}(MgADP)_2$ for free $Kp1^\dagger$. Increasing the $[Kp2]/[Kp1]$ ratio will therefore decrease the degree of inhibition at a given total protein concentration. Thirdly, the $[MgATP]/[MgADP]$ ratio and concentrations will not only effect the kinetics of reduction of oxidized Fe protein (Yates *et al.*, 1975) but will also modulate the electron-transfer rate between reduced $Kp2$ and $Kp1$ (Thorneley & Cornish-Bowden, 1976; Hageman *et al.*, 1980).

H₂ evolution as a function of [Kp2]/[Kp1] ratio (titration curves)

The standard assay, which is used to determine the specific activities of the component proteins that comprise nitrogenase isolated from various diazotrophs, involves the measurement of H_2 -evolution or C_2H_2 -reduction rates as a function of the $[Kp2]/[Kp1]$ ratio. The concentration of the protein whose specific activity is being determined is kept constant and the concentration of the complementary protein is varied. The maximum rate of substrate reduction obtained in the 'titration curve' is then used to calculate the specific activity of the protein whose concentration was kept constant (Eady *et al.*, 1972). Eady & Postgate (1974) and Emerich *et al.* (1981) have reviewed the literature of titration curves, and, although they recognized that the stoichiometry and kinetics of complex-formation between the Fe protein and MoFe protein, the rates of reduction of oxidized Fe protein by the electron donor and the nature of the reducible substrate were all important parameters, they could not present either a comprehensive qualitative explanation or quantitative simulation of the shape of these curves.

Scheme 2 and the rate constants in Table 1 of Lowe & Thorneley (1984a) can simulate both types of titration curve quantitatively and provide an explanation for the variation in the shape of these curves as various parameters are changed.

(a) *Titration of Kp1 with Kp2.* Fig. 3 shows data that constitute a typical titration curve such as is used to determine the specific activity of MoFe protein. The $Kp1$ concentration was kept constant and the $Kp2$ concentration increased. The specific activity of the $Kp1$ is calculated from the limiting

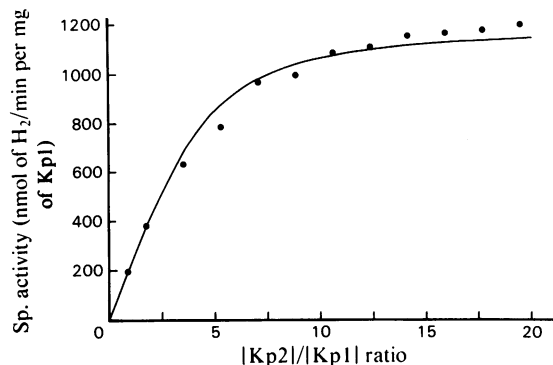


Fig. 3. *Titration of Kp1 with Kp2*

The data points were obtained by using the standard assay procedure described in the Methods and materials section with $[Kp1] = 0.53 \mu M$ and $[Kp2]$ varied as shown. The continuous line is a simulation obtained by using Table 1 and Scheme 2 of Lowe & Thorneley (1984a).

rate of H_2 evolution at high $[Kp2]/[Kp1]$ ratio. The maximum specific activity occurs when the rate of dissociation of $Kp2_{ox.}(MgADP)_2$ from $Kp1^\dagger$ ($k_{-3} = 6.4 \pm 0.8 s^{-1}$) is rate-limiting and a value of 1760 ± 220 nmol of H_2 /min per mg of $Kp1$ can be calculated at $23^\circ C$. This calculation assumes that $Kp1$ contains two independent substrate reduction sites, each of which involves 1 Mo atom. Several factors can cause a lower rate of H_2 evolution, as follows.

(1) The specific activity will be proportional to the Mo content of the $Kp1$ (Hawkes *et al.*, 1984).

(2) Inhibition at low and high protein concentrations, as discussed above.

(3) When $[Kp2] < [Kp1^\dagger]$, a low specific activity for $Kp1$ results because the rate of H_2 evolution equals $k_{-3}[Kp1-Kp2_{ox.}(MgADP)_2]$, and the concentration of this complex cannot exceed the total $Kp2$ concentration, which is less than that of $Kp1^\dagger$. If all the $Kp2$ is active, the maximum specific activity for $Kp1$ will result when $[Kp2] = [Kp1^\dagger]$, provided that the rate of reduction of $Kp2_{ox.}(MgADP)_2$ (determined by the concentration of $S_2O_4^{2-}$ and k_4) is fast compared with the rate of complex-formation between $Kp2_{ox.}(MgADP)_2$ and $Kp1^\dagger$ (k_{+3}). This latter reaction is also responsible for the inhibition observed at high protein concentrations. Increasing the concentration of $S_2O_4^{2-}$ will overcome this inhibition (see section below on the dependence of activity on $S_2O_4^{2-}$ concentration).

(4) Inhibition is also caused by the competition between inactive $Kp2$ and active $Kp2(MgATP)_2$ for $Kp1^\dagger$. Our ability to simulate the data in Fig. 3 further justifies our assumption (Lowe & Thorne-

ley, 1984a; Thorneley & Lowe, 1984) that Kp2₁ binds to and dissociates from Kp1[†] with the same rate constants (*k*₊₃ and *k*₋₃) as does active Kp2_{ox}(MgADP)₂. Thus the shape of the titration curve will depend on the activity of the protein used. Increasing the concentration of S₂O₄²⁻ will not decrease the inhibition due to inactive Fe protein. However, increasing the [Kp2]/[Kp1] ratio does decrease the inhibition, since active reduced Kp2(MgATP) binds essentially irreversibly to Kp1[†], whereas the binding of inactive Kp2 is reversible. Thus, the higher the activity of Kp2 and Kp1, the tighter the curvature of the titration curve and the maximum activity will be achieved closer to the limiting [Kp2]/[Kp1] ratio of 2:1. It is not possible to achieve this limiting situation in practice with S₂O₄²⁻ as the electron donor, since a significant proportion of the Kp2 will be present as Kp2_{ox}(MgADP)₂ (determined by the value of *k*₄ and the low concentration of SO₂⁻). The use of Na₂S₂O₄ concentration above 50mM is precluded by salt effects (Thorneley & Lowe, 1983). In

protein. The Kp2 concentration was kept constant and the Kp1 concentration was increased.

The reasons for the shape of this curve are the same as those discussed above for the Kp1 titration curve. The inhibition that is observed at a high [Kp1]/[Kp2] ratio is due to the back-reaction involving Kp2_{ox}(MgADP)₂ binding to Kp1[†] (*k*₊₃) competing effectively with the rate of reduction of Kp2_{ox}(MgADP)₂ by SO₂⁻ (*k*₄). Increasing the rate of reduction of Kp2_{ox}(MgADP)₂ will therefore decrease the extent of this inhibition. The limitations on increasing this reduction rate by increasing the concentration of S₂O₄²⁻ were discussed above. However, Hageman & Burris (1978) have achieved relief of the inhibition by excess of MoFe protein by addition of flavodoxin.

The maximum specific activity of Kp2 protein can be calculated from *k*₋₃ = 6.4 ± 0.8s⁻¹ to be 2860 ± 360nmol of H₂/min per mg of Kp2 at 23 °C. The maximum specific activities (Sp. act.) of the Fe protein and MoFe protein for H₂ evolution are related by eqn. (2):

$$\text{Sp. act. of Fe protein} = \frac{\text{Sp. act. of MoFe protein}}{2} \times \frac{M_r \text{ of MoFe protein}}{M_r \text{ of Fe protein}} \quad (2)$$

addition, when [Na₂S₂O₄] is greater than 50mM, the rate of reduction of Kp2_{ox}(MgADP)₂ becomes independent of [S₂O₄²⁻], which may mean that release of MgADP or an associated conformation change in the protein becomes rate-limiting (Thorneley, & Lowe, 1983).

(b) *Titration of Kp2 with Kp1*. Fig. 4 shows data points that constitute a typical titration curve such as is used to determine the specific activity of Fe

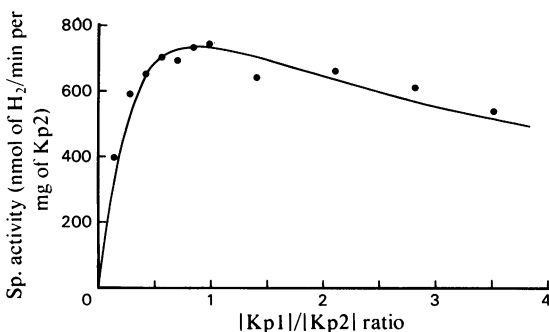


Fig. 4. *Titration of Kp2 with Kp1*

The data points were obtained by using the standard assay procedure described in the Methods and materials section with [Kp2] = 0.92 μM and [Kp1] varied as shown. The continuous line is a simulation obtained by using Table 1 and Scheme 2 of Lowe & Thorneley (1984a).

This relationship requires that the Fe protein transfers one electron to one of two independently functioning substrate reduction sites on the MoFe protein and that the rate-limiting step is the dissociation of oxidized Fe protein from MoFe protein, which occurs after each electron transfer (Thorneley & Lowe, 1983). The simulation in Fig. 4 assumed that the Kp2 protein was 45% active. By using the maximum specific activity of 2860 ± 360nmol of H₂/min per mg of Kp2 calculated above, Kp2 that was 45% active might be expected to give a measured maximum specific activity in the titration curve shown in Fig. 3 of 1290nmol of H₂/min per mg of Kp2. The maximum activity obtained experimentally was only 800nmol of H₂/min per mg of Kp2. The limitation of dithionite as a reductant and the inhibition by inactive Kp2 account for the difference. Thus the ratio of measured specific activity of Fe protein to theoretical maximal specific activity underestimates the percentage of the total Fe protein that is active. This is also illustrated by data for Kp nitrogenase proteins obtained at 30°C, the temperature most commonly used for assaying nitrogenase. The simulations made by Lowe & Thorneley (1984a,b) and Thorneley & Lowe (1984) required the Kp2 protein, used to obtain the data, which had a measured activity at 30°C of 1500nmol of H₂/min per mg of Kp2, to be only 45% active. Thus fully active Kp2 might be expected to have a specific activity of 3300 nmol of

H_2 /min per mg of Kp2. However, using eqn. (2) and a value of 2500 ± 500 nmol of H_2 /min per mg for the specific activity of Kp1 (Hawkes *et al.*, 1984) gives a value of 4000 ± 800 nmol of H_2 /min per mg for the maximum specific activity of Kp2. The difference is due to the effect of inactive Kp2. As the percentage of the total Fe protein that is active increases, the difference will become less significant.

Dependence of the rate of H_2 evolution on $S_2O_4^{2-}$ concentration

It is generally agreed that $SO_2^{\cdot-}$ is the true electron donor to nitrogenase when dithionite is the reductant (Thorneley & Lowe, 1983). There is, however, some controversy as to whether the dependence shows saturating (Hageman & Burris, 1978) or non-saturating (Watt & Burns, 1977) kinetics. Scheme 2 and Table 1 of Lowe & Thorneley (1984a) can be used to explain the observations made by Hageman & Burris (1978) that the apparent K_m for $S_2O_4^{2-}$ decreases as the Fe protein/MoFe protein ratio increases. At the higher component-protein ratios a lower concentration of $S_2O_4^{2-}$ is required to maintain a sufficient steady-state concentration of reduced Fe protein; this is one of the explanations given by Hageman & Burris (1978). However, the quantitative prediction of our scheme indicates that dependence is not hyperbolic, although as the Fe protein/MoFe protein ratio increases the deviations from hyperbolic behaviour become smaller. These effects are illustrated in Fig. 5, which shows good agreement between the experimentally obtained data and the simulations. The concept of an apparent K_m for dithionite is therefore not valid,

although experimental limitations on dithionite concentrations can produce apparently hyperbolic curves.

The simulations also predict a dependence on absolute protein concentration. As the protein concentrations increase, the dependence becomes more parabolic (i.e. the intercept on a reciprocal plot tends to zero). This effect is more apparent at low dithionite concentrations. It is to be noted that Watt & Burns (1977) observed a parabolic dependence for particulate partially purified *Azotobacter vinelandii* nitrogenase. The discrepancy in the form of the dependence between the work of Hageman & Burris (1978) (hyperbolic) and Watt & Burns (1977) (parabolic) could be due either to enhanced values of k_{+1} (and k_{+3} ?), or to locally elevated protein concentrations, within the complex. If, as this view suggests, the protein association and dissociation rates are altered within active particulate nitrogenase, it might be possible to explain the results reported by Haaker *et al.* (1984), who estimated an Fe-protein specific activity *in vivo* of 7000 nmol of C_2H_2 reduced/min per mg of Fe protein after O_2 shock of an *Azotobacter vinelandii* culture.

We were pleased when the scheme correctly predicted the form of the protein titration curves. It was only after a detailed inspection of the computer-simulated concentrations of the various intermediates that we recognized the precise origin of, for instance, the inhibition of H_2 evolution at high MoFe protein/Fe protein ratio. Although the scheme is the simplest one that we are able to construct for a dissociating nitrogenase system that involves eight sequential electron transfers, kinetic complexity is inherent in a scheme defining 17 rate

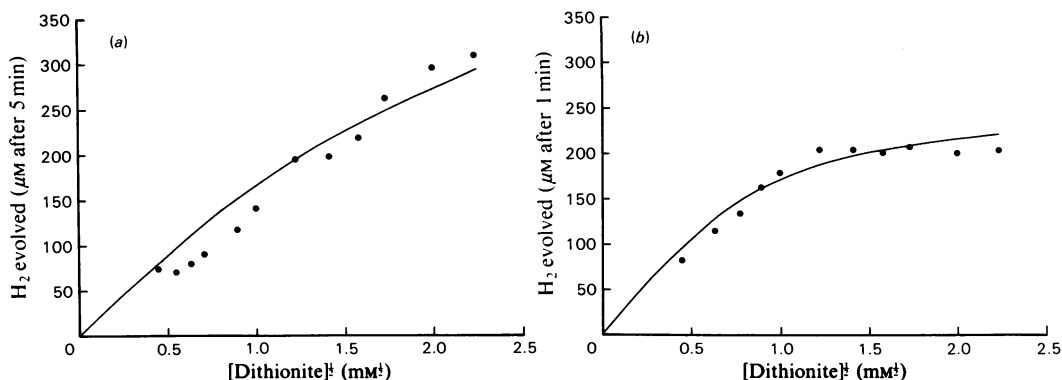


Fig. 5. Dependence of the rate of H_2 evolution from nitrogenase on dithionite concentration. The data points were obtained as described in the Methods and materials section. Total amounts of H_2 evolved at (a) 5 min and (b) 1 min are plotted because of non-linearity in the assays at low dithionite concentrations. The protein concentrations were: (a) $[Kp1] = 1.7 \mu M$ and $[Kp2] = 1.8 \mu M$; (b) $[Kp1] = 1.7 \mu M$ and $[Kp2] = 9.0 \mu M$. The lines are simulations obtained by using Table 1 and Scheme 2 of Lowe & Thorneley (1984a).

constants and 46 intermediates. The ability to simulate experiments is satisfying; the prospect of predicting the response of the system to changed parameters is exciting.

We thank Professor J. R. Postgate for comments on the manuscript, Mr. K. Baker, Miss L. Sones and Mr. S. D. Harrison for provision of *Klebsiella pneumoniae* cells, and Mr. K. Fisher and Mrs. G. Ashby for skilled technical assistance.

References

- Dilworth, M. J. & Thorneley, R. N. F. (1981) *Biochem. J.* **193**, 971–983
- Eady, R. R. & Postgate, J. R. (1974) *Nature (London)* **249**, 805–810
- Eady, R. R., Smith, B. E., Cook, K. A. & Postgate, J. R. (1972) *Biochem. J.* **128**, 655–675
- Eady, R. R., Issack, R., Kennedy, C., Postgate, J. R. & Ratcliffe, H. D. (1978) *J. Gen. Microbiol.* **104**, 277–285
- Emerich, D. W., Hageman, R. V. & Burris, R. H. (1981) *Adv. Enzymol. Relat. Areas Mol. Biol.* **52**, 1–22
- Haaker, H., Braaksma, A., Cordewener, J., Klugkist, J., Wassink, H., Grande, H., Eady, R. & Veeger, C. (1974) in *Advances in Nitrogen Fixation Research* (Veeger, C. & Newton, W. E., eds.), pp. 123–131, Nijhoff-Junk, The Hague, Boston and Lancaster
- Hageman, R. V. & Burris, R. H. (1978) *Biochemistry* **17**, 4117–4124
- Hageman, R. V., Orme-Johnson, W. H. & Burris, R. H. (1980) *Biochemistry* **19**, 2333–2342
- Hawkes, T. R., McLean, P. A. & Smith, B. E. (1984) *Biochem. J.* **217**, 317–321
- Hennecke, H. & Shanmugam, K. T. (1979) *Arch. Microbiol.* **123**, 259–265
- Lowe, D. J. & Thorneley, R. N. F. (1984a) *Biochem. J.* **224**, 877–886
- Lowe, D. J. & Thorneley, R. N. F. (1984b) *Biochem. J.* **224**, 895–901
- Mortenson, L. W. (1964) *Proc. Natl. Acad. Sci. U.S.A.* **52**, 272–279
- Roberts, G. P., MacNeil, T., MacNeil, D. & Brill, W. J. (1978) *J. Bacteriol.* **136**, 267–269
- Thorneley, R. N. F. & Cornish-Bowden, A. (1977) *Biochem. J.* **165**, 255–262
- Thorneley, R. N. F. & Lowe, D. J. (1983) *Biochem. J.* **215**, 393–403
- Thorneley, R. N. F. & Lowe, D. J. (1984) *Biochem. J.* **224**, 887–894
- Thorneley, R. N. F., Eady, R. R. & Yates, M. G. (1975) *Biochim. Biophys. Acta* **403**, 269–284
- Watt, G. D. & Burns, A. (1977) *Biochemistry* **16**, 264–270
- Yates, M. G., Thorneley, R. N. F. & Lowe, D. J. (1975) *FEBS Lett.* **60**, 89–93